Journal of Metals, Materials and Minerals, Vol.28 No.2 pp.94-105, 2018

Effect of chromium content on the three-body-type abrasive wear behavior of multi-alloyed white cast iron

Jatupon OPAPAIBOON[1], Mawin SUPRADIST NA AYUDHAYA[1,*], Prasonk SRICHAROENCHAI[1], Sudsakorn INTHIDECH[2] and Yasuhiro MATSUBARA[3]

[1]*Department of Metallurgical Engineering, Faculty of Engineering, Chulalongkorn University, Bangkok, 10330, Thailand*
[2]*Department of Manufacturing Engineering, Faculty of Engineering, Mahasarakham University, Mahasarakham, 44150, Thailand*
[3]*National Institute of Technology, Kurume College, Kurume, Fukuoka, 830-8555, Japan*

***Corresponding author e-mail:** Mawin.S@chula.ac.th

Received date:
7 June 2018
Revised date:
27 September 2018
Accepted date:
12 October 2018

Keywords:
Multi-alloyed white cast iron
Hardness
Retained austenite
Three-body-type abrasive wear behavior
Cr effect

Abstract

The effect of Cr content on three-body-type abrasive wear behavior of multi-alloyed white cast iron was investigated. Multi-alloyed white cast irons were prepared with varying Cr content from 3-9 mass% under basic alloy composition. Annealed specimens were hardened from 1323 and 1373K austenitizing and tempered at three levels of temperatures which were at maximum hardness (H_{Tmax}), lower and higher than that at H_{Tmax} (L-H_{Tmax} and H-H_{Tmax}). A rubber wheel wear tester was used to evaluate the abrasive wear resistance. The hardness and volume fraction of the retained austenite (V_γ) varied depending on Cr content and heat treatment condition. The linear relation between wear loss and wear distance was obtained in all specimens. In each heat treatment condition, the wear rate (R_w) value decreased to 6 mass%Cr, and then, increased gradually as Cr content increased. As-hardened specimens showed higher wear resistance than tempered specimens did. In tempered state, the lowest R_w was obtained in H_{Tmax} specimen and the highest in L-H_{Tmax} or H-H_{Tmax} specimens. The R_w lowered greatly as the macro-hardness rose to 830 HV30, and after that it decreased continuously as the hardness increased. Moreover, R_w scattered broadly at V_γ lower than 5%, and then, decreased gradually as V_γ rose.

1. Introduction

Multi-alloyed white cast irons have been developed as materials resistant to abrasive wear for about 30 years. The main purpose is to improve the abrasive wear resistance and toughness of parts or machine components in the mining, cement and steel industries. This cast iron contains plural types of carbide forming elements such as chromium (Cr), molybdenum (Mo), tungsten (W) and vanadium (V). The eutectic carbides formed in the multi-alloyed white cast iron include MC, M_2C or M_6C and M_7C_3 types [1-3]. It was reported that the rolling mill rolls made by multi-alloyed white cast iron showed much higher wear performance than the conventional rolls made by Ni-hard and high Cr cast irons [2]. Thus far, multi-alloyed white cast irons have been mainly applied to hot work rolls in steel-making plants and some for pulverizing mill parts in the mining and cement industries.

The basic alloy composition of multi-alloyed white cast iron is 5 mass% (hereafter mass% is expressed by %) of each Cr, Mo, W and V [3,4]. In addition, cobalt (Co) is added to improve the properties such as hardness and toughness at a high temperature. During solidification, the primary austenite (γ_P) solidifies first and followed by eutectic reaction of (γ+carbide). The type and morphology of carbide crystallizes from liquid depending on the kind and the amount of carbide formers and the solidification rate [4]. On the other side, the heat treatment of the alloys after solidification is very important because the matrix structures which are related to the mechanical or wear properties can be controlled and modified [5].

Generally, the heat treatment of multi-alloyed white cast iron consists of annealing, hardening and tempering processes in the same way as high Cr cast iron and tool steel [2]. During holding at the austenitizing temperature, the austenite is destabilized by the precipitation of secondary

DOI: 10.14456/jmmm.2018.32

carbides, and then, transforms to martensite or bainite during cooling to room temperature. The precipitation of special carbides due to carbide reaction occurs during tempering at a high temperature. The retained austenite left after tempering can also be transformed into martensite during post cooling. As a result, the matrix with high hardness and better wear resistance are formed.

In industrial applications, the abrasive wear can be classified into two-body and three-body-types [5-8]. In the case of three-body-type abrasive wear, the abrasive particles move freely on the surface of materials. An example of this wear condition can be found in the ball mills or the tube mills to pulverize the cement clinker. The suitable test equipment to evaluate the wear resistance of three-body-type abrasion is a rubber wheel abrasive wear tester [5,9].

The abrasive wear behavior in the industrial application is very complex and varies according to the wearing environment, type of abrasives, contacting angle, magnitude of applied load and the microstructure of materials [6,10]. With respect to the abrasive wear resistant cast alloys, it is essential to clarify the effects of alloying element and heat treatment condition on the microstructure and wear resistance. This could lead to success in the practical applications of the industrial field.

It is well known that Cr is not as strong of a carbide former as the other elements like Mo, W or V. However, Cr forms the discontinuous morphology of eutectic M_7C_3 carbide which increases the toughness [3, 5-8] and dissolves in the matrix to improve the hardenability of the cast iron significantly. Therefore, Cr is added in multi-alloyed white cast form in the interest of hardenability.

The research on solidification sequence and heat treatment behavior of multi-alloyed white cast irons has already been reported for basic alloy composition [11,12]. However, systematic research on the abrasive wear behavior related to heat treatment condition has not yet been conducted. In this study, therefore, the effect of Cr content on the abrasive wear resistance of heat-treated multi-alloyed white cast irons was investigated using a rubber wheel (three-body-type) abrasive wear tester. Then, the correlations among Cr content, hardness, retained austenite, heat treatment condition and abrasive wear resistance were clarified.

2. Experimental

Charge calculation for target chemical composition was carried out to each specimen using raw materials such as mild steel, pig iron, ferro-alloys and pure metals. The charge materials were melted down in a high frequency induction furnace and superheated to 1853K. After holding at that temperature, each melt was poured at a temperature between 1763 and 1793K into preheated CO_2 molds of which the cavity shape was a Y-block and sufficient riser as shown in Figure 1 (a). The surface of the top riser was immediately covered with dry exothermic powder to prevent the liquid of the risers from rapid cooling. The riser was cut off and a substantial block with the size of 50x50x200 mm, as shown in Figure 1 (b), was supplied to annealing for removing the inner stress and micro-segregation produced during solidification. The block was coated with an anti-oxidation paste to prevent oxidation and decarburization during annealing. The block was annealed at 1223K for 18 ks and cooled in the furnace. After annealing, the block was sectioned at 7 mm in thickness by a wire-cutting machine to obtain test pieces shown in Figure 1 (c). The chemical compositions of the specimens are shown in Table 1.

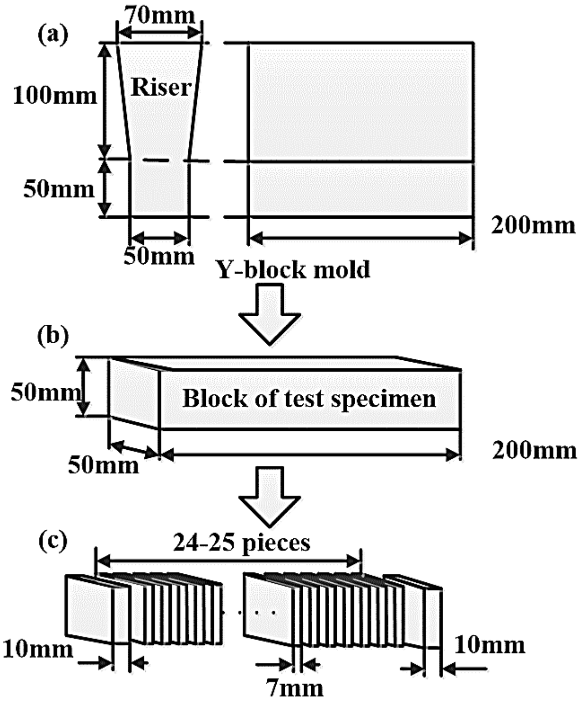

Figure 1. Process to prepare test pieces.

Table 1. Chemical compositions of the specimens.

Specimen	**Element (mass%)**							
	C	**Si**	**Mn**	**Cr**	**Mo**	**W**	**V**	**Co**
No.1 (3%Cr)	1.96	0.52	0.49	3.09	5.02	5.02	4.96	1.98
No.2 (5%Cr)	1.97	0.52	0.52	4.98	5.02	4.98	5.07	1.99
No.3 (6%Cr)	2.02	0.54	0.51	5.99	4.93	4.93	4.97	2.00
No.4 (7%Cr)	1.98	0.50	0.49	7.01	5.09	5.05	5.03	2.01
No.5 (9%Cr)	2.08	0.53	0.49	8.93	5.01	5.03	5.07	2.00

Table 2. Tempering temperatures connected to heat treatment conditions.

Specimen	**Tempering temperature (K)**					
	1323K austenitizing			**1373K austenitizing**		
	L-H$_{Tmax}$	**H$_{Tmax}$**	**H-H$_{Tmax}$**	**L-H$_{Tmax}$**	**H$_{Tmax}$**	**H-H$_{Tmax}$**
No.1 (3%Cr)	748	798	827	748	798	827
No.2 (5%Cr)	748	798	827	748	798	840
No.3 (6%Cr)	723	773	820	723	773	840
No.4 (7%Cr)	723	773	827	723	773	827
No.5 (9%Cr)	723	773	810	723	773	827

The test pieces were austenitized at 1323K and 1373K in a vacuum furnace and held there for 3.6 ks. After holding, the test pieces were hardened by fan air cooling (FAC) to room temperature. As-hardened specimens (As-H) were tempered at three levels of temperatures selected on the tempered hardness curve which had already been obtained experimentally, at the temperature necessary for the maximum tempered hardness (H_{Tmax}), and lower and higher temperatures than that at H_{Tmax} (L-H_{Tmax} and H-H_{Tmax}, respectively). The tempering temperature is summarized in Table 2. The holding time was 12 ks and cooled to room temperature in the air.

The microstructure was observed using an optical microscope (OM) and scanning electron microscope (SEM). The test pieces were polished using emery paper and buffed with 0.1 μm alumina powder. Groesbeck's, Murakami's and Villella's reagents were adopted to reveal the microstructure. The hardness of the specimen was measured using Vickers hardness tester with a load of 294.2 N (30 kgf) for macro-hardness and 0.98 N (0.1 kgf) for micro-hardness, respectively. In each specimen, the hardness was randomly measured at five points and average values were adopted.

The volume fraction of retained austenite (V_γ) was measured using an X-ray diffraction method. The rotating and swinging goniometer with special sample stage enabled the test piece to cancel the effect of the preferred crystal orientation of austenite. The X-ray beam source was Mo-K_α characteristic line with a wavelength of 0.0711 nm. The scanning range was from 24 to 44 degrees by 2θ. For quantitative calculation, $(200)_\alpha$ and $(220)_\alpha$ planes for ferrite (α) or martensite as $(220)_\gamma$ and $(311)_\gamma$ planes for austenite (γ) were adopted, respectively. The image analyzer program was used to integrate the area under each peak. The $V_\gamma$value was calculated from three combinations of peaks, $(220)_\alpha$-$(311)_\gamma$, $(200)_\alpha$-$\Sigma(220,311)_\gamma$ and $\Sigma(200,220)_\alpha$-$(311)_\gamma$ and the average value was adopted.

The surface roughness (Ra-max) of the specimen was controlled at less than 1 μm using a grinding machine. The schematic drawing of rubber wheel abrasive wear tester is illustrated in Figure 2. The silica sand of AFS 60 grade was used as the abrasive material. The sand was fed at approximately 250-300 g/min to the contacting face of the rotating rubber wheel with 250 mm in diameter and the surface of the test piece. The test was conducted at a rotation speed of 120 rpm under the load of 85.32 N (8.7 kgf). The rubber wheel rotated in the same direction as the flow of the abrasives. At every 1000 revolutions, the weight loss of the test piece was measured using a high precision digital balance with 0.1 mg accuracy. The test was continued repeatedly for four times on the same area of the worn surface.

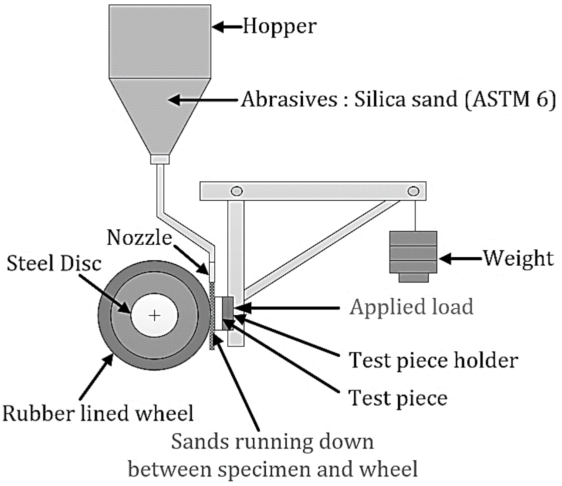

Figure 2. Schematic drawing of rubber wheel abrasion wear tester.

3. Results and Discussion

3.1 Microstructure of test specimens

Typical microstructures of test specimens in the as-cast state are shown in Figure 3. All specimens show hypoeutectic structure consisting of primary austenite dendrite and eutectic structures. The type and morphology of eutectic carbide in multi-alloyed white cast iron was studied by Wu et al. [13] and Hashimoto et al. [13]. They reported that the crystallized eutectic carbides were MC, M_2C and M_7C_3 types. The MC carbide has nodular morphology while the M_2C carbide shows fine lamellar morphology. By contrast, the eutectic M_7C_3 carbide was rod-like or ledeburitic morphology and sometime co-existed with MC and M_2C carbides. It is well known that these carbides can be distinguished by Murakami's and Groesbeck's reagents. That is to say, both tint or color the M_2C and M_7C_3 carbides but do not for MC carbide [1]. Therefore, it is clear that the eutectic carbides in Figure 3 were MC type with some M_2C and/or M_7C_3 types depending on the Cr content.

The eutectic carbides in specimens with Cr content lower than 6% were mainly MC and M_2C types. In the specimen with 6%Cr, the eutectic carbides were MC and M_2C coexisting with a reasonable number of M_7C_3 types. As for the specimens with Cr content more than 6%, the eutectic carbides were mostly MC and M_7C_3 types. Therefore, it can be said that the 6%Cr inhibited the (γ+M_2C) eutectic and instead it promoted the crystallization of (γ+M_7C_3) eutectic. Matrices of all the specimens are mostly austenitic. This is because Cr as well as other alloying elements dissolve into the matrix stabilized austenite and lower the Ms temperature [14].

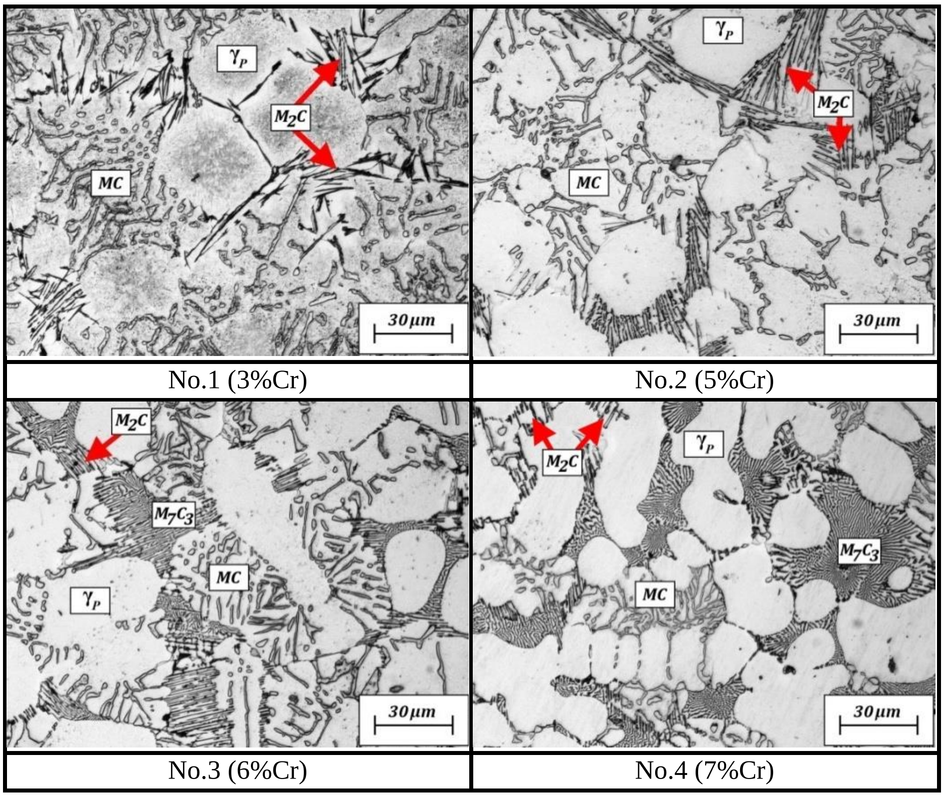

No.1 (3%Cr)

No.2 (5%Cr)

No.3 (6%Cr)

No.4 (7%Cr)

Figure 3. As-cast microstructures of specimens with different Cr contents.

Table 3. Area fractions of primary austenite (γ_P) and eutectic structures.

Specimen	Primary austenite (%)	Eutectic structure (%)		
		γ+MC	$\gamma+M_2C$	$\gamma+M_7C_3$
3%Cr	58.27	40.56	1.17	-
5%Cr	56.43	34.21	9.36	-
6%Cr	58.14	32.02	5.97	3.87
7%Cr	54.75	27.51	-	17.74
9%Cr	55.68	22.82	-	21.50

In order to clarify how Cr content affects the fraction of crystallized phases from the liquid, the area fractions of each phase were quantitatively measured by an image analysis software and the results are summarized in Table 3. Even if the Cr content increased greatly, the area fraction of primary austenite (γ_P) changed a little in the range of only 54% to 58%. When considering the effect of Cr content on individual eutectic structure, it was found that the area fraction of (γ+MC) eutectic decreased orderly from 40.56% in 3%Cr specimen to 22.82% in 9%Cr specimen. The value of ($\gamma+M_2C$) eutectic increased to the highest value of 9.36% in 5%Cr specimen, and then, it decreased to 5.97% in 6%Cr specimen. On the other side, the area fraction of ($\gamma+M_7C_3$) eutectic increased greatly from 3.87% in 6%Cr specimen to 21.50% in 9%Cr specimen.

It is known that the hardening process has little effect on eutectic carbide [11-13]. By contrast, it gives great effect on the matrix structure. For example, the SEM microstructures of specimens hardened from 1373K austenitizing are displayed in Figure 4. This is evident from high magnification that the matrices of all the specimens are composed of fine secondary carbides (Sc), martensite (M) and retained austenite (γ_R). In the as-cast matrix structure shown in Figure 3, however, the precipitation of carbides cannot be found at all. This proves that the destabilization of austenite, i.e., precipitation of secondary carbides, occurred during austenitizing and then, residual austenite transformed into martensite during quenching. As for the precipitated secondary carbides in the matrix, the types of carbides cannot be identified using of OM, SEM and XRD but only by TEM because the carbide sizes are very fine. However, it was reported that the precipitated secondary carbides in heat-treated multi-alloyed white cast iron with basic alloy composition were MC, M_6C and M_7C_3 types [15]. From the microphotographs of as-hardened specimens, the difference in the amount of secondary carbides among the specimens is not clear even the Cr content of specimens varied. However, it seems that the amount of retained austenite is greatest in the specimens with 5 and 6%Cr.

3.2 Effect of Cr content on hardness and volume fraction of retained austenite (V_γ) of heat-treated specimens

The hardness and V_γ of all the specimens were measured. The relations of Cr content and hardness as well as V_γ of specimens hardened from 1323K austenitizing are shown as examples in Figure 5 and Figure 6, respectively. It was found that the hardness and V_γ varied depending on the heat treatment condition and Cr content. The macrohardness shows similar variation to micro-hardness, i.e., hardness increased to 5%Cr and then decreased with the rise of Cr content. The reason of a rise in hardness of as-hardened state is due to that an increase in Cr dissolved in matrix strengthens the matrix and promotes the precipitation of secondary carbides. Another reason is that the Cr delays pearlite and bainite transformations and improves the hardenability of the cast iron. The decreasing of the hardness in the latter stage causes according to an increase in the amount of ($\gamma+M_7C_3$) eutectic with lower hardness than those of (γ+MC) and ($\gamma+M_2C$) eutectics. In each heat treatment, the hardness in the as-hardened state was greater than those in the tempered state.

The hardness in each tempering temperature showed similar trend to that of the as-hardened state. An increase in Cr promotes the precipitation of secondary carbides during tempering and then increases the hardness. At the same Cr content, the hardness of H_{Tmax} specimen are naturally higher than those of the L-H_{Tmax} and H-H_{Tmax} specimens. The reason is that the matrix of H_{Tmax} specimen mainly composed of secondary carbides and martensite with small amount of retained austenite. The highest tempered hardness (H_{Tmax}) was obtained from the specimen with 5 to 6%Cr in both of austenitizing temperatures.

The effect of Cr content on the V_γ is shown in Figure 6. The V_γ in as-hardened state increased gradually to the highest value at 5%Cr and then decreased slowly. At the former stage, the Cr dissolved in austenite lowered the Ms temperature and consequently, the V_γ increased. At the latter stage, the V_γ continued to decrease because the Ms temperature in multi-alloyed white cast iron increases as the Cr content rises over 5% [14]. The V_γ value is overall high in the case of high austenitizing temperature of 1373K, and there, the solubilities of C and alloying elements in austenite were increased. These elements dissolved more in austenite depressed the Ms temperature. The V_γ value in the as-hardened state is naturally higher than that in the tempered state. In the tempered state, the V_γ value of L-H_{Tmax} specimen is reasonably higher than those of H_{Tmax} and H-H_{Tmax} specimens.

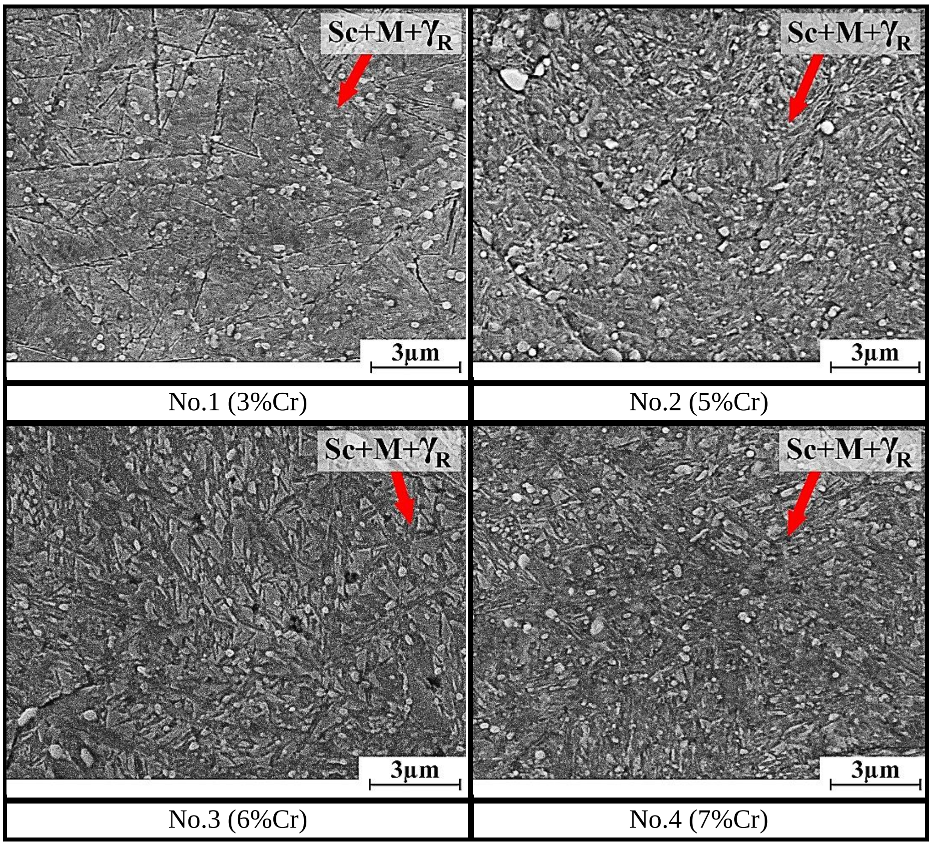

No.1 (3%Cr)
No.2 (5%Cr)
No.3 (6%Cr)
No.4 (7%Cr)

Figure 4. SEM microphotographs of specimens hardened from 1373K austenitizing.

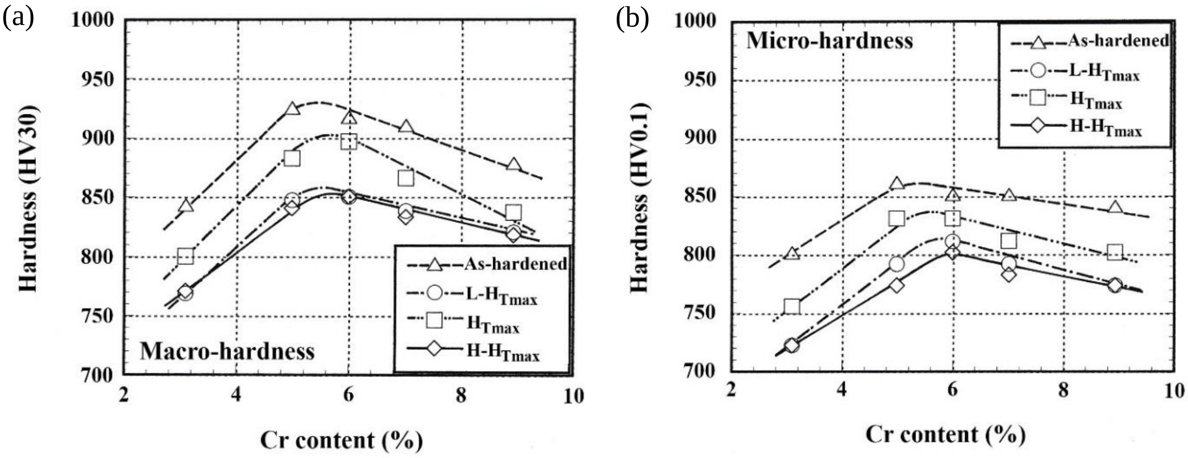

Figure 5. Effect of Cr content on macro-hardness (a) and micro-hardness (b) of specimens with different heat treatment conditions. Austenitizing temperature: 1323K.

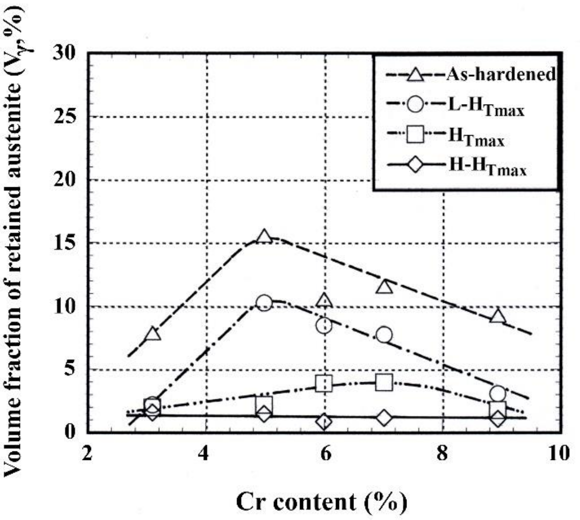

Figure 6. Effect of Cr content on volume fraction of retained austenite (V_γ) of specimens with different heat treatment conditions. Austenitizing temperature: 1323K.

3.3 Abrasive wear behavior

As mentioned earlier, the multi-alloyed white cast iron has been developed for the hot rolling mill rolls. During operation, the surface of roll is worn by abrasive materials. Consequently, the main properties required are hardness and toughness of cast iron which determines the wear resistance. Therefore, factors enhancing the wear resistance can be the hardness and the toughness of cast iron. It is known that the retained austenite has high ductility and closely related to the toughness of the cast iron. In addition, the retained austenite is work-hardened during service and it improves the wear resistance of the cast iron as well.

The relationship between wear loss (W_l) and wear distance (W_d) of specimens No. 1 to No. 4 hardened from 1323K austenitizing are representatively displayed in Figure 7. In all diagrams, the wear loss increases in portion to the wear distance regardless of Cr content and heat treatment conditions. The wear loss is the largest in the specimen tempered at L-H_{Tmax}, and the smallest is obtained in as-hardened specimens. Since the linear relation was obtained in all the specimens, the wear rate (R_w, mg/m) which is expressed by the slope of each straight line is calculated to evaluate the abrasive wear resistance.

3.3.1 Effect of Cr content on wear rate (R_w)

The effect of Cr content on R_w is shown in Figure 8 (a) for 1323K and (b) for 1373K austenitizing, respectively. The R_w value decreases to the lowest at 6%Cr and at over 6%Cr it continues to increase contrarily. This trend is opposite to hardness and shows similar behavior even if the austenitizing temperature and heat treatment conditions are varied. However, the R_w values are overall smaller in the specimens hardened from a high austenitizing temperature of 1373K. When the R_w values are individually viewed by heat treatment condition, the R_w of as-hardened specimen (As-H) is lower than those of tempered specimens at the same Cr content.

From this point, the effect of Cr content on the R_w shall be explained. It has been clarified that the wear resistance increases alongside an increase in the Cr content up to 6%. The reason can be explained by the fact that the Cr improves the hardenability and at the same time, it decreases the Ms temperature until 5~6%Cr [14]. Therefore, the amount of retained austenite in the as-hardened state rises with an increase in Cr content up to 6% and it contributes more to the precipitation of carbides, i.e., more secondary hardening in tempered state. Simultaneously, an increase in retained austenite could promote more transformation of martensite in tempering process. When the Cr content gets over 6%, on the contrary, the opposite trend to the behavior of R_w with Cr content less than 6% appears. This could be due to a reduction of hardness with increasing the Cr content. An increase in Cr content promotes the precipitation of eutectic M_7C_3 and secondary $M_{23}C_6$ carbides with lower hardness than that of MC, M_2C and M_6C carbides. In addition, the retained austenite in the as-hardened state decreases because the Ms temperature increases with an increase in the Cr content over 6% [14]. Consequently, the secondary hardening is lowered during tempering.

All over the Cr content, the wear mechanism in this three-body-type wear test is considered as follows: the hardness of abrasive particles (silica) are about 1200 HV and lower than those of eutectic carbides with 1500-3000 HV [2]; therefore, the matrix region with lower hardness is worn preferentially. As mentioned above, it can be understood that the matrix hardness must be a major factor to the abrasive wear resistance.

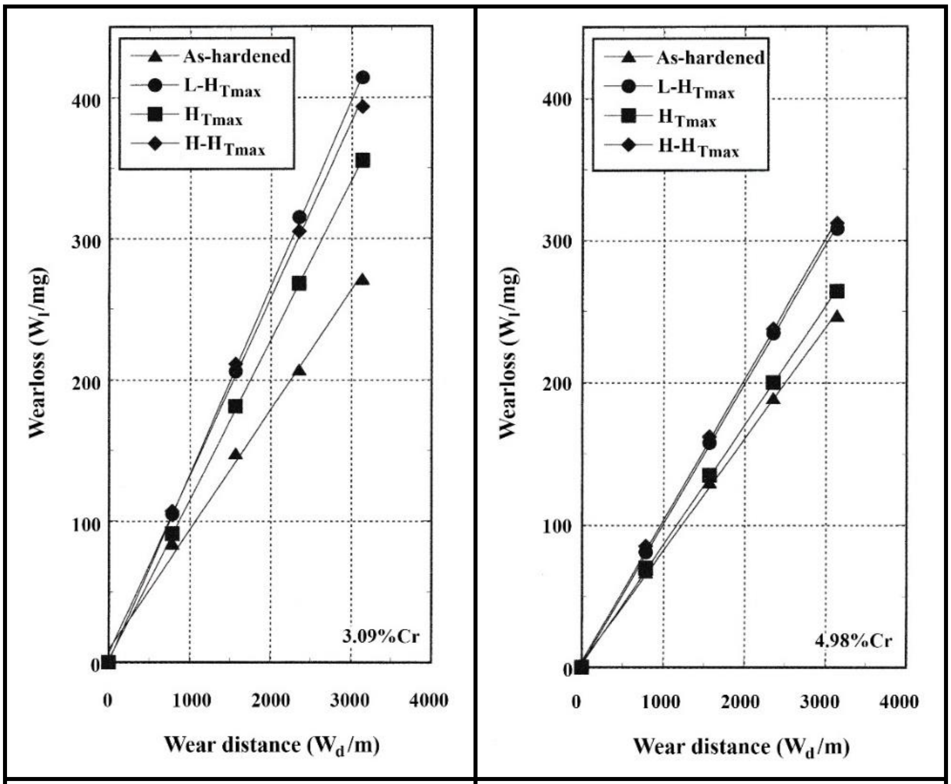

No.1 (3%Cr) No.2 (5%Cr)

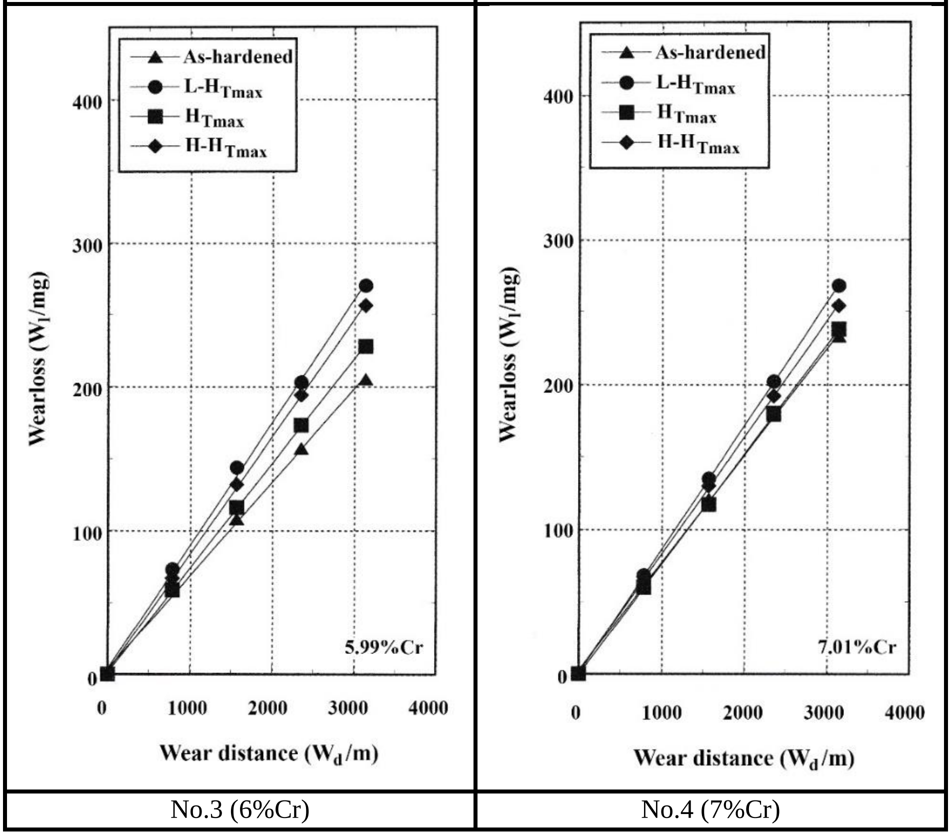

No.3 (6%Cr) No.4 (7%Cr)

Figure 7. Relationship between wear loss (W$_l$) and wear distance (W$_d$) of specimens hardened from 1323K austenitizing.

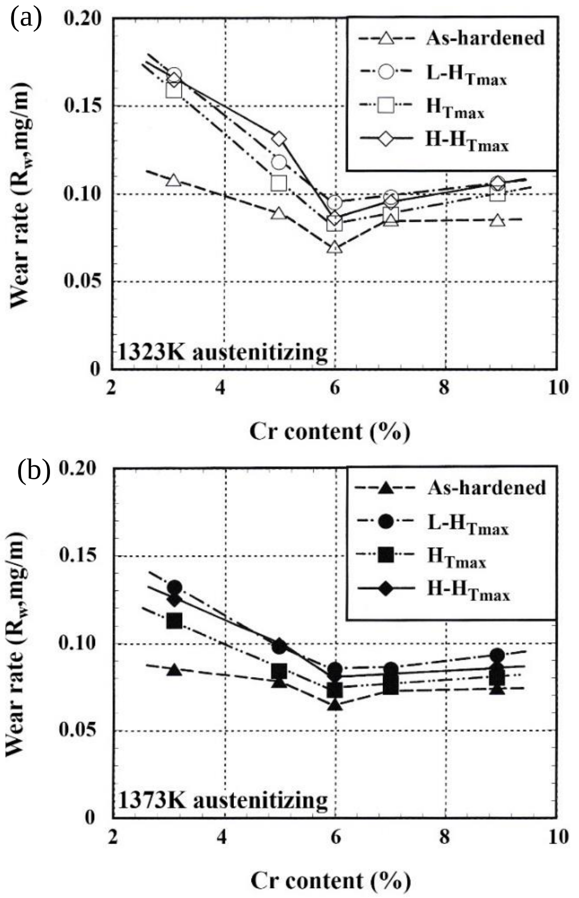

Figure 8. Effect of Cr content on wear rate (R_w) of specimens with different heat treatment conditions. Austenitizing temperature: (a) 1323K and (b) 1373K.

Here, the reasons why As-H specimen shows better wear resistance than tempered specimens are discussed by focusing on the matrix structure. The phases existing in the matrix are quite different between as-hardened and tempered states even if the hardness is similar. In the as-hardened state, the matrix consists of secondary carbides precipitated during austenitizing, high carbon martensite caused by quenching and austenite remained without transformation. In the tempered state, on the other hand, the matrix of H_{Tmax} specimen has very fine tempered martensite, secondary carbides and some retainedaustenite, and H-H_{Tmax} specimen have coarse carbides, tempered martensite and very less retained austenite. By contrast, the L-H_{Tmax} specimen has tempered martensite and more retained austenite than H-H_{Tmax} specimen. Consequently, the R_w of As-H specimen with higher matrix hardness than those in tempered specimens shows the lowest R_w values in each Cr specimen. In the tempered state, it is reasonable that the H_{Tmax} specimens should show the lowest R_w value or highest wear resistance, followed by H-H_{Tmax} and L-H_{Tmax} specimens. It is noted that the difference in matrix structure between as-hardened and tempered specimens determined the difference in hardness or wear resistance.

From the viewpoint of difference in the R_w value, it may be considered that the As-H specimens may supply practical rolls and parts or components necessary to abrasive wear resistance. However, it will be accompanied by some risks in one meaning because a large amount of retained austenite can be transformed to martensite involving a great deal of expansion and this could certainly cause cracking or destruction of the products while using.

3.3.2 Effect of hardness on wear rate (R_w)

In alloyed white cast iron, the hardness is interconnected with the types and amounts of eutectic and secondary carbides precipitated in the matrix. It is said that the precipitated carbides make the matrix strong by an effect of dispersion strengthening. The relationships between R_w and macro-hardness as well as micro-hardness are shown in Figure 9 (a) and (b), respectively.

The R_w values decrease steeply as the hardness increases to 830 HV30 for macro-hardness and 780 HV0.1 for micro-hardness. At over each hardness, the R_w values continue to decrease gradually. This indicates that higher hardness provides better wear resistance on the whole. In the former stage, the remarkable decrease in the R_w could be due to an increase in the matrix hardness. The matrix hardness of heat-treated specimens rises due to an increase in the precipitated secondary carbides and martensite. This behavior leads to the improvement of wear resistance. In the latter stage, hardness over 830 HV30 gives a small effect on the R_w. It is considered that the R_w is determined by the hardness involving work-hardening of retained austenite. In As-H specimens, the retained austenite is stabilized by saturation of alloying elements. It is reported that the stress in the three-body-type wear test is quite low [16] and therefore, the work-hardening of austenite was rather small in this experiment. With respect to wear behavior, an increase in retained austenite promotes pitting and scratching wore on the matrix and too high hardness made the matrix brittle and posed a risk of spalling wear additionally. For this reason, the R_w decreases a little even if the hardness is increased. As for the difference in austenitizing temperature, higher austenitizing temperature provides a lower R_w value because more austenite formed in the as-hardened state and precipitated more secondary carbides during tempering, and more martensite formed by cooling after tempering.

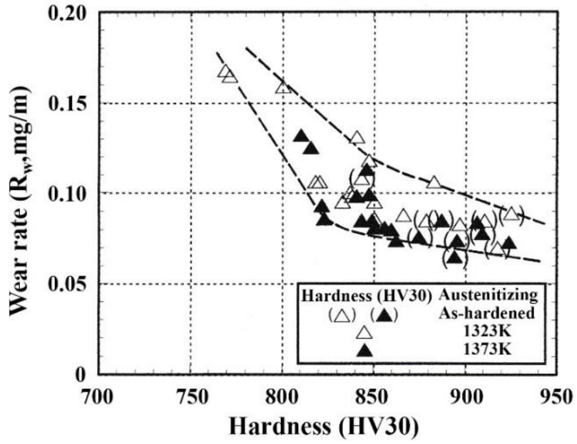

(a) Macro-hardness

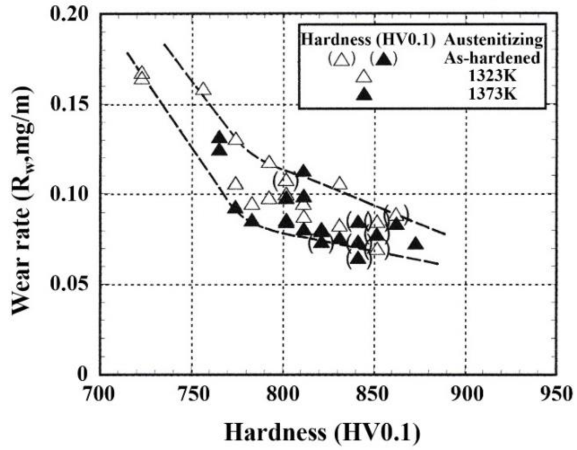

(b) Micro-hardness

Figure 9. Relationship between wear rate (R_w) and hardness of specimens. (a) Macro-hardness and (b) Micro-hardness.

3.3.3 Effect of retained austenite on wear rate (R_w)

From the previous results, it is clear that the R_w varies significantly according to the transformation of retained austenite (γ_R). The relationship between V_γ and R_w is shown in Figure 10. It is found that the R_w can be separated into two groups: the first group is the tempered specimens with less than 5%V_γ and the second one is almost As-H specimens with over 5%V_γ. In the first group, the R_w scattered widely regardless of V_γ values. Within this range of V_γ, the R_w is influenced by the hardness rather than V_γ value and the higher hardness provides the lower R_w. In the second group in which V_γ is more than 5%, the R_w decreases slowly. As described in the section of hardness vs. R_w, the work-hardening of retained austenite in this wear test is small, and this suggests that the work-hardening will not improve the R_w significantly. However, there is a report in which it was found that a large amount of austenite decreased the matrix hardness and increased the R_w [16]. Within this level of retained austenite in the experiment, the effects mentioned just above must be low, and if the retained austenite is contained much more than in the specimens for this experiment, the hardness should decrease and the R_w value must rise.

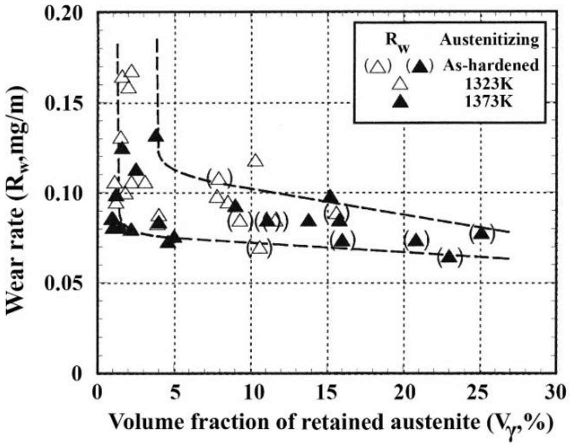

Figure 10. Relationship between wear rate (R_w) and volume fraction of retained austenite (V_γ) of specimens.

3.3.4 Observation of worn surface by SEM

The worn surface appearances of 5%Cr specimen hardened from 1373K austenitizing was investigated by SEM with different magnifications and the microphotographs are shown in Figure 11. Unlike the two-body-type abrasion wear test, the worn direction cannot be observed as shown in Figure (a). Instead, the traces of grooving wear (G) on the eutectic region and scratching ones (S) on the matrix can be observed as shown in Figure (b). In addition, many pitting or spalling wears (P) are found in the matrix as shown by high magnification microphotograph in Figure (c). Therefore, it can be said that under the three-body-type abrasive wear test, grooving, scratching and pitting or spalling wears take place simultaneously all over the surface.

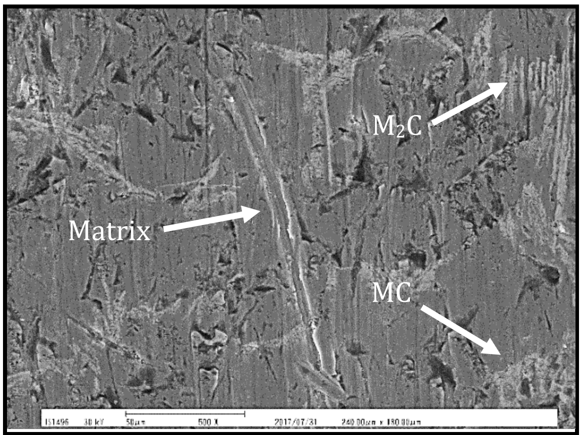

(a) Worn surface

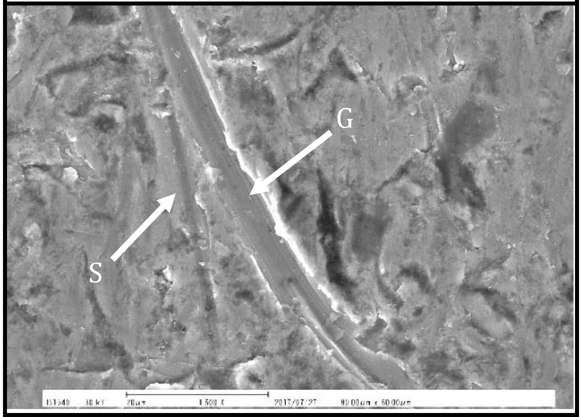

(b) Grooving (G) and Scratching (S)

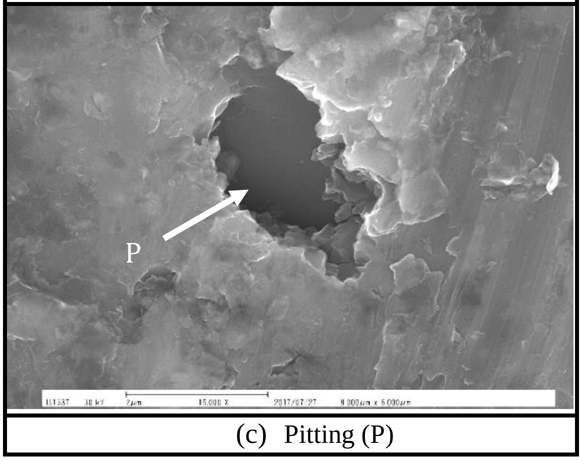

(c) Pitting (P)

Figure 11. SEM microphotographs of worn surfaces of 6%Cr specimen hardened from 1373K.

4. Conclusions

Three body-type abrasive wear tests of heat-treated multi-alloyed white cast irons with 3-9%Cr in basic alloy composition were carried out. After annealing, the specimens were hardened from 1323 and 1373K austenitizing and tempered at three levels of temperatures: a temperature giving the maximum hardness (H_{Tmax}), and lower and higher temperatures than that at the H_{Tmax} (L-H_{Tmax}, H-H_{Tmax}, respectively). The effects of hardness, volume fraction of retained austenite (V_γ) and Cr content on wear behavior were clarified connecting with heat treatment conditions. The conclusions are summarized as follows:

1. A linear relation was obtained between wear loss (W_l) and wear distance (W_d) irrespective of heat treatment conditions and Cr contents.
2. In all specimens, the lowest wear rate (R_w) or largest wear resistance was obtained in the as-hardened specimen (As-H) and followed by the H_{Tmax} specimen. The wear resistance of the L-H_{Tmax} specimen was the smallest.
3. The R_w of specimen in each heat treatment condition decreased gradually to 6%Cr and at over 6%Cr it continued to increase.
4. The R_w decreased as the hardness increased to 830 HV30, and over that, it continued to decrease gradually. The higher austenitizing temperature provided the smaller R_w or larger wear resistance.
5. From relation of Rw vs. V_γ of all specimens, the R_w was separated into two groups at 5%V_γ. The R_w scattered widely in the range of V_γ less than 5%. At over 5%V_γ, the R_w decreased a little as the V_γ increased.
6. The wear direction could not be observed on the worn surface but scratching and pitting wears were distinguished.
7. The highest wear resistance was obtained in the specimens with 6%Cr regardless of austenitizing temperatures.

5. Acknowledgement

The authors appreciate Chulalongkorn University for financial support through the fund of "The 100th Anniversary Chulalongkorn University for Doctoral Scholarship" and "Overseas Research Experience Scholarship for Graduate Student". In addition, we would like to thank the Manufacturing and Metallurgical Engineering Research Unit of the Faculty of Engineering at Mahasarakham University, the Cast Metals Laboratory of the National Institute of Technology at Kurume College, Thai Parkerizing Co., Ltd. and Isobe Iron Works Co., Ltd. for usage of their experimental equipment.

References

[1] H.-Q. Wu, N. Sasaguri, Y. Matsubara, and M. Hashimoto, "Solidification of multi-alloyed white cast iron : Type and morphology of carbides," *AFS Transactions,* vol. 140, pp. 103-108, 1996.

[2] M. Hashimoto, "Development of multi-component white cast iron (HSS) rolls and rolling technology in steel rolling," *Abrasion Wear Resistant Alloyed White Cast Iron for Rolling and Pulverizing Mills,* pp. 1-23, 2008.

[3] Y. Matsubara, N. Sasaguri, and M. Hashimoto, "The history and development of cast rolls for hot working mill," *The 4th Asian Foundry Congress-Australia,* pp. 251-261, 1996.

[4] M. Boccalini Jr., "Overview : High speed steels for hot rolling mill rolls," *Abrasion Wear Resistant Alloyed White Cast Iron for Rolling and Pulverizing Mills,* pp. 123-142, 2011.

[5] I. R. Sare and B. K. Arnold, "The influence of heat treatment on the high-stress abrasion resistance and fracture toughness of alloy white cast irons," *Metallurgical and Materials Transactions A,* vol. 26, no. 7, pp. 1785-1793, 1995.

[6] G. Laird, R. Gundlach, and K. Rohrig, *Abrasion-Resistance Cast Iron Handbook.* USA: American Foundry Society, 2000.

[7] J. D. Watson, P. J. Mutton, and I. R. Sare, "Abrasive wear of white cast irons," *Australian Institute of Metals Forum,* vol. 3, pp. 74-88, 1980.

[8] K.-H. Zum Gahr and D. V. Doane, "Optimizing fracture toughness and abrasion resistance in white cast irons," *Metallurgical Transactions A* vol. 11, no. 4, pp. 613-620, 1980.

[9] S. Ma, J. Xing, Y. He, Yefei Li, Z. Huang, G. Liu, and Q. Geng, "Microstructure and crystallography of M_7C_3 carbide in chromium cast iron," *Materials Chemistry and Physics,* vol. 161, pp. 65-73, 2015.

[10] O. Kubo, M. Hashimoto, and Y. Matsubara, "Influence of microstructure on wear resistance and crack propagation characteristics required for white iron rolling mill rolls," *Proceedings of The Science of Casting and Solidifications,* 2001.

[11] J. Opapaiboon, P. Sricharoenchai, S. Inthidech, and Y. Matsubara, "Effect of carbon content on heat treatment behavior of multi-alloyed white cast iron for abrasive wear resistance," *Materials Transections,* vol. 56, no. 5, pp. 720-725, 2015.

[12] W. Khanitnantharak, M. Hashimoto, K. Shimizu, K. Yamamoto, N. Sasaguri, and Y. Matsubara, "Effects of carbon and heat treatment on the hardness and austenite content of a multi-component white cast iron," *AFS Transactions,* vol. 117, pp. 435-444, 2009.

[13] M. Hashimoto, O. Kubo, and Y. Matsubara, "Analysis of carbides in multi-component white cast iron for hot rolling mill rolls," *ISIJ International,* vol. 44, no. 2, pp. 372-380, 2004.

[14] Y. Yokomizo, N. Sasaguri, K. Nanjo, and Y. Matsubara, "Relationship between continuous cooling transformation behavior and chromium content of multi-component white cast iron," *Journal of Japan Foundry Engineering Society,* vol. 74, no. 11, pp. 691-698, 2002.

[15] M. Hashimoto, O. Kubo, N. Sasaguri, and Y. Matsubara, "Analysis of precipitated carbides in matrix of multi-component white cast iron," *Journal of Japan Foundry Engineering Society,* vol. 76, no. 3, pp. 205-211, 2004.

[16] A. Chooprajong, P. Sricharoenchai, S. Inthidech, and Y. Matsubara, "Three-body-type abrasive wear behavior of 26% Cr cast iron with molybdenum," *Journal of Metals, Materials and Minerals,* vol. 22, pp. 31-37, 2012.